GEOFIZIKA VOL.6 1989

Preliminary communication
UDC 551.521.32

A model of radiative heat transfer effects in the atmospheric boundary layer

Darko Koračin, Branko Grisogono** and Nebojša Subanović***

**Hydrometeorological Institute of SR Croatia, Zagreb*

***Geophysical Institute, Faculty of Science, University of Zagreb, Yugoslavia*

Received 13 June 1986, in final form 10 May 1988.

During nighttime clear-sky conditions and in the absence of significant advection the influence of divergence of net longwave radiative flux on thermodynamic processes could be dominant in the atmospheric boundary layer. The model which parametrizes such processes by height (35 grid points up to 2000 m) is accomplished based on the emissivity concept.

The test of the model is performed on the Wangara experiment data. The results are analysed and discussed concerning a complex structure of the atmospheric boundary layer. The modeled radiative cooling rate is comparable with the total cooling rate, especially in the lower part of the nocturnal boundary layer (region of smaller wind speeds).

Model efekata radijacijskog prijenosa topline u graničnom sloju atmosfere

Za vedrih noći i bez značajne advekcije dominantan je utjecaj divergencije neto dugovalnog zračenja na termodinamičke procese graničnog sloja atmosfere. Razvijen je model na konceptu emisivnosti koji parametrizira takve procese po visini (35 točaka mreže sve do 2000 m).

Model je testiran na Wangara podacima. Dobiveni rezultati analizirani su i razmotreni u skladu s kompleksnošću strukture graničnog sloja atmosfere. Modelirani iznos radijacijskog ohlađivanja usporediv je s ukupnim iznosom ohlađivanja, osobito u nižem dijelu noćnog graničnog sloja (područje manje brzine vjetra).

1. Introduction

Cooling of the atmospheric boundary layer during nighttime clear sky conditions and without significant advection, is governed by turbulent flux divergence and net radiative flux divergence. In the case of weak advection and nonsignificant spatial inhomogeneities, thermodynamic equation shows balance of this effects:

$$\frac{\partial \Theta}{\partial t} = \frac{\partial \left(\overline{-w' \Theta'}\right)}{\partial z} + \frac{1}{\rho C_p} \frac{\partial F_N}{\partial z} \tag{1}$$

where:

Θ - mean potential temperature of the air
$\overline{-w'\Theta'}$ - vertical temperature flux
ρ - air density
C_p - specific heat at constant air pressure
$F_N = F_D - F_U$ net longwave radiative flux
F_D - downward longwave flux
F_U - upward longwave flux.

During nighttime, clear sky condition net-radiative flux divergence becomes important, or even dominant term in (1) (see e.g. Kondratyev, 1972; Garratt and Brost, 1982; André and Mahrt, 1982).

It appears that the radiative flux divergence is usually neglected in numerical boundary layer modelling (Delage, 1974; Wyngaard, 1975; Brost and Wyngaard, 1978; Zeman, 1979). Some studies have dealt with both terms – turbulent and radiative heat flux divergences (e.g. André et al., 1978; Yamada and Mellor, 1975; Nieuwstandt, 1980) and some with radiative heat transfer only (e.g. Brunt, 1934; Anffosi et al., 1976; Klöppel et al., 1978).

2. Model concept

Parametrization of net longwave radiative flux divergence is based on the "emissivity concept" (e.g. Paltridge and Platt, 1976; Pielke, 1984).

Downward longwave flux from infinity to the considered height z is:

$$F_D(z) = \int_z^{\infty} B\,[T(z')]\,\frac{\partial E(z',z)}{\partial z'}\,\mathrm{d}z' \qquad (2)$$

where:

B - Stefan - Boltzmann law (σT^4)
T - air temperature,
σ - Stefan - Boltzmann constant,
$E(z', z)$ - emissivity due to corrected mass of absorber u, from z to z' (procedure for emissivity calculation is presented in the Appendix),
z' - dummy integration variable.

One of the main absorbers of longwave radiation in the atmosphere is water vapor and u can be expressed as:

$$u(z) = C_1 \int_{z_0}^{z} q(p/p_0)^{C_2}\,\mathrm{d}z' \qquad (3)$$

with the following symbols:

z_0 - roughness length considering radiative heat transfer (smaller or equal to roughness length considering transfer of momentum),
p_0 = 1000 mb,

p - actual air pressure,
$C_1 = 1$ (Garratt and Brost, 1982; André and Mahrt, 1982; Bodin, 1978),
C_2 - pressure term correction coefficient, usually in the range from 0.5 to 1.0. Garratt and Brost (1982) as well as André and Mahrt (1982) use 0.9 (also used in our work. It may be mentioned that Houghton (1977, p.140-142) presents various empirical results and fits C_2 to 0.675,
q - mixing ratio.

Upward longwave flux to the considered height z is:

$$F_U(z) = \int_z^{z_o} B[T(z')] \frac{\partial E(z,z')}{\partial z'} \, dz' + [1 - E(z,z_o)] E_o \sigma T_o^4 + + C_3 (1 - E_o) F_{D,o} [1 - E(z,z_o)] \tag{4}$$

with:

E_o - surface emissivity,
T_o - surface temperature,
C_3 - surface reflectivity of the longwave radiative flux, $0 \lesssim C_3 \lesssim 1$,
$F_{D,o}$ - total incoming longwave radiative flux at the surface.

We are neglecting the third term on the right hand side of eq. (4) - it is the least of the three ($0 < E_o < 1$ and $0 < C_3 < 1$ in our problems).

After the calculus transformation (e.g. Pielke, 1984; p 187-199) one can obtain the final expression for radiative cooling contribution to the boundary layer thermodynamic processes:

$$\left(\frac{\partial \Theta}{\partial t}\right)_R = \frac{q}{C_p} (p/p_o)^{0.9} \left[4\sigma \left(- \int_{T(z)}^{T(z_r)} T'^3 \frac{\partial E(u',u)}{\partial u} \, dT' + + \int_{T(z)}^{T(z_o)} T'^3 \frac{\partial E(u,u')}{\partial u} \, dT' \right) - (1 - E_o) \sigma T_o^4 \frac{\partial E(u,0)}{\partial u} \right] \tag{5}$$

The first term on the right hand side represents the flux due to absorption of longwave radiation in the corrected mass of water vapor from the considered level to the top of the model. The second term represents flux due to absorption of longwave radiation in the corrected mass of water vapor from the ground to the considered level z. Third term is due to the gray - body radiative emission of surface to the considered level z.

3. Computer calculation

In order to solve (5) numerically the transformation from integral to discrete scheme has to be performed. Transformed eq. (5) is:

$$\left(\frac{\Delta\Theta_i}{\Delta t}\right)_{rad} = \frac{q}{C_p} (p/p_0)^{0.9} \left[-4\sigma \sum_{j=i}^{n-1} \frac{dE(u_{j+1/2}-u_i)}{du_i} T^3_{j+1/2} (T_{j+1}-T_j) + \right. \tag{6}$$

$$\left. + 4\sigma \sum_{j=i}^{1} \frac{dE(u_i-u_{j-1/2})}{du_i} T^3_{j-1/2} (T_{j-1}-T_j) - (1-E_0)\,\sigma T^4 \frac{dE(u_i)}{du_i} \right]$$

where:

$i = 1, 2, \ldots n$ ($n = 35$ in our model),

$\dfrac{dE(u_i)}{du_i}$, $\dfrac{dE(u_i-u_{j-1/2})}{du_i}$, $\dfrac{dE(u_{j+1/2}-u_i)}{du_i}$ - are given in the Appendix.

We can see corresponding terms in (5) and (6), respectively.

One of the novelties in this work are analytic functions for $(dE(u)/du_i)$ and their direct taking into account of net radiative flux divergence (without longwave radiative flux calculus). Consequently, the computer program is shorter and obtained results are in better agreement with the experimental data.

4. Data base: Wangara experiment

The radiative cooling model has been tested against Wangara experiment data (Clarke et al., 1971). During July and August 1967 great scientific expedition was conducted in Australia near town Hay (43° 30' S, 144° 56' E) in the open, smooth terrain.

One of the aims of the Wangara experiment was to investigate the boundary layer. Four measuring stations were positioned approximately at the corners of a square with a side of about 60 km and the fifth one was close to its center. The station referred to as number 5 was representative for the very smooth terrain ($z_0 = 1.20 \pm 0.10$ mm) while the station referred to as number 4 was representative for the cotton bush vegetation with z_0 from 6.0 to 20.3 mm. The Wangara experiment measurements consisted of:

- hourly pilot balloon winds averaged over the five stations (up to 2 km),
- radiosonde data at the station 5 (every 3 hours),
- micrometeorological measurements at the stations 4 and 5,
- surface observations (pressure, dry and wet bulb temperature, surface wind direction),
- estimation of the surface geostrophic wind,
- thermal winds and total acceleration at 500 m height.

Micrometeorological measurements at the station 5 included wind speed measured on the mast at 0.5, 1, 2, 4, 8 and 16 m height, temperature differences between 1 and 2 m, and 2 and 4 m, net radiation and ground heat flux measurements.

At the station 4 there were wind measurements on the same levels, except 0.5 m, because of somewhat rougher surroundings.

5. Grid structure of the model

To take into consideration the real behaviour of the vertical profiles of the boundary layer parameters with stronger gradients close to the ground (approximately corresponding to log-curves) and lower gradients in greater heights (approximately corresponding to lin-curves), the transformed coordinate should be introduced. A differential spacing between successive new coordinate (z') has to be inversely proportional to the turbulent exchange coefficient $K(z)$:

$$dz' = \frac{1}{K(z)} dz \tag{7}$$

Using the fact that the turbulent coefficient is proportional to the neutral mixing length (l_n):

$$K = l_n / D$$

where D is a constant, and the expression for l_n:

$$\frac{1}{l_n} = \frac{1}{kz} + \frac{1}{F}, \qquad z_o \leq z \tag{8}$$

where:

k - von Kármán constant (0.35),

F - a constant chosen to be a fraction of the depth of the boundary layer model (H): $F = aH$ (a is a constant, usually 0.2),

the expression for z' is finally:

$$z' = D\,[(1/k)\ln(z/z_o) + \frac{z - z_o}{F}] + 1 \tag{9}$$

The constant D can be determined from the condition for specified number of gridpoints and from the condition: $z' = 1$ for $z = z_o$, ($D \approx 0.32$), and by taking into account that a step in z' is equal to one.

The height of 2000 m has been chosen for the top of the model with 35 points in vertical spacing which is usually sufficient (Bodin, 1978).

6. Initialization of the model

Radiosonde data (wind, temperature and humidity profiles) start from 2 m height and an extrapolation to the roughness length z_o has to be performed. On the basis of the similarity theory, the result of André et al. (1978) for Monin – Obukhov height L ($L \approx$ 1 m, for the Wangara night 33 - 34) and flux-gradient relationships (Businger et al., 1971), have been used in extrapolation.

Humidity scale q_* has been determined from the equation for surface energy balance together with measured net radiation and ground heat flux.

A linear interpolation has been used on the input data between 2 and 50 m, and Lagrangian polynom from 50 m to the top of the model.

On the top of the model all input data are assumed constant; such assumption is real in our case and very useful when we calculate longwave radiative flux divergence directly.

7. Model results

Input data for the model calculation are the Wangara experiment data (Day 33–34) on 00.19 Eastern Australian Time (EAT).

Computer program based on the described algorithms (Section 2 and 3) has been installed on the UNIVAC 1110 computer. At each level upward and downward contributions of corrected mass of water vapor (Figs. 1 and 2), emissivities (Figs. 3 and 4) and divergence of net longwave radiative flux have been determined. Nonlinear shapes of such curves is obvious indicating complex influence of air temperature, density and humidity in the atmospheric boundary layer.

Radiative cooling rate is basically estimated in K/sec, extrapolated for an hour (K/h) and presented in Fig. 5. This cooling rate is comparable with previous simulations (e.g. André and Mahrt, 1982; Fig. A1.). In Fig. 6 we have reconstructed the results from André and Mahrt with simultaneously depicted results from our simulation. The results are satisfactory and encouraging. Cooling rate in this simulation is variable in the lowest layer and reaches the maximum (0.48 K/h) at the height below the first inversion (about 50–70 m). Deviation of the cooling rate close to the ground is probably caused by non-inclusion of the surface energy balance equation related to the lower boundary condition.

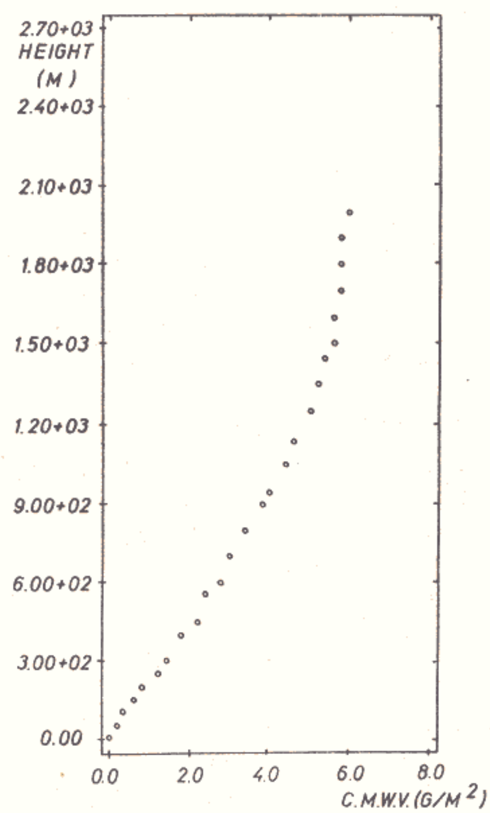

Figure 1. Upward corrected mass of water vapor versus height.

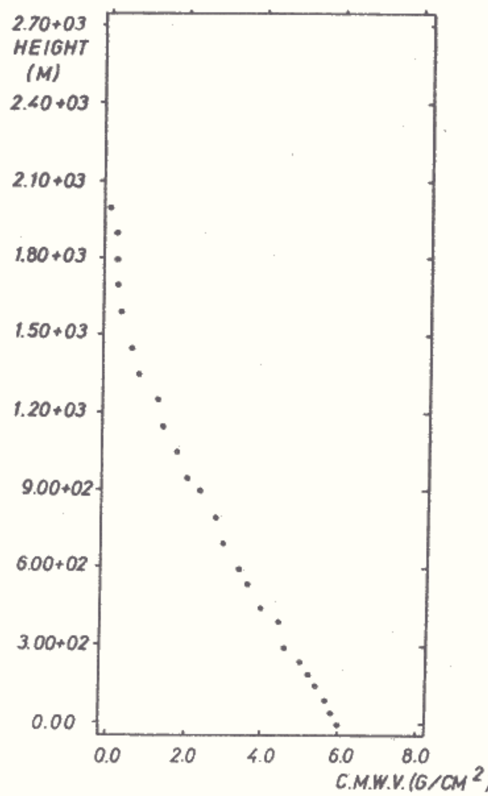

Figure 2. Downward corrected mass of water vapor versus height.

Above the height of the surface inversion, cooling rate is gradually decreasing and becomes negligible beyond approximately 900 m. From Fig. 6 it can also be seen that the "shift" between these two curves in higher region is obtained, but the amount of the shift is only about 0.05 K/h except in the mentioned lowest part. This difference is mainly caused by the inclusion of additional absorber - CO_2 (André and Mahrt, 1982) which can augment the cooling rate. CO_2 concentration is usually taken as constant by height, while the water vapor influence decreases by height (decrease of mixing ratio by height). This is the reason why the cooling rate in our model tends to zero in greater heights, while results of André and Mahrt still retain cooling rate of about 0.1 K/h aloft (above 600 m).

Using the friction velocity (u_*) and the Coriolis parameter (f) one can estimate turbulent boundary layer height by the diagnostic relation:

$$h_t = c\, u_* \, / f$$

where c is a constant (usually 0.3).

In this case (Wangara 33-34, 00.19 EAT) turbulent boundary layer height is about 150 m. From Fig. 6 it can be seen that the main variations of the divergence of the net longwave radiative flux are below 100 m (the height of the near ground inversion and the beginning of the isothermal layer, 100 - 300 m height). Therefore, one can conclude that the depth of the turbulent boundary layer caused by mechanical influence is close to the depth of the main influence of the divergence of the net longwave flux (except the shallow layer approximately few meters close to the ground).

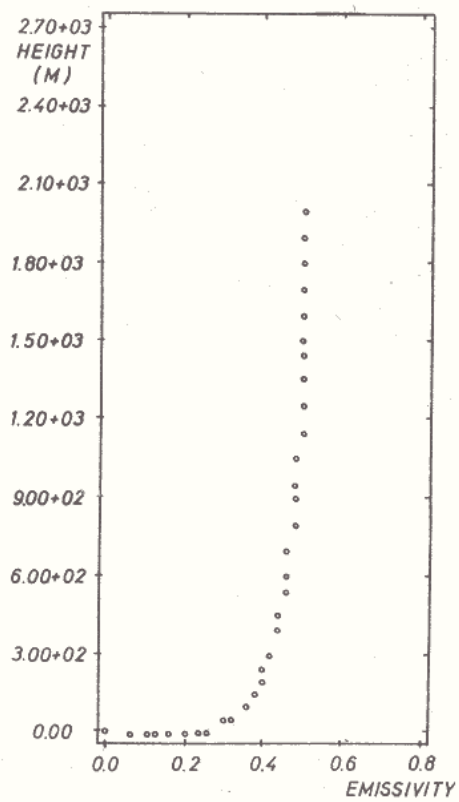

Figure 3. Emissivity due to water vapor in the upward corrected mass of water vapor versus height.

8. Concluding remarks

The model of the atmospheric boundary layer caused by the divergence of the net longwave radiative flux has been established. The algorithms of the model are based on the emissivity concept.

Computer calculations are performed in 35 grid points up to 2000 m in vertical direction, considering real structure of the nocturnal atmospheric boundary layer. The discretization of the analytic derivation of emissivity and direct calculation of longwave radiative flux divergence is used in our work, instead of the usually used finite difference approximation for the emissivity derivation and derivation in divergence of the radiative flux.

The model is tested against the Wangara experiment data (night 33-34). The results are in accordance with physical behaviour of the boundary layer parameters. The comparison of this model to other similar simulations (e.g. André and Mahrt, 1982) is encouraging and the main differences can be explained.

The influence of the CO_2 absorber as well as interaction terms (water vapor with CO_2, also with aerosols, ...) should be taken into account in the future development of the model.

The model should be incorporated in the complete boundary layer model with both turbulent and radiative heat transfer effects and also with dynamical effects concerning advection and terrain influence.

Acknowledgment

The authors are particularly indebted to Dr. Nadežda Šinik for constructive advice.

Appendix

Emissivity $E(u)$ is calculated as follows (Bodin, 1978, Pielke, 1984):

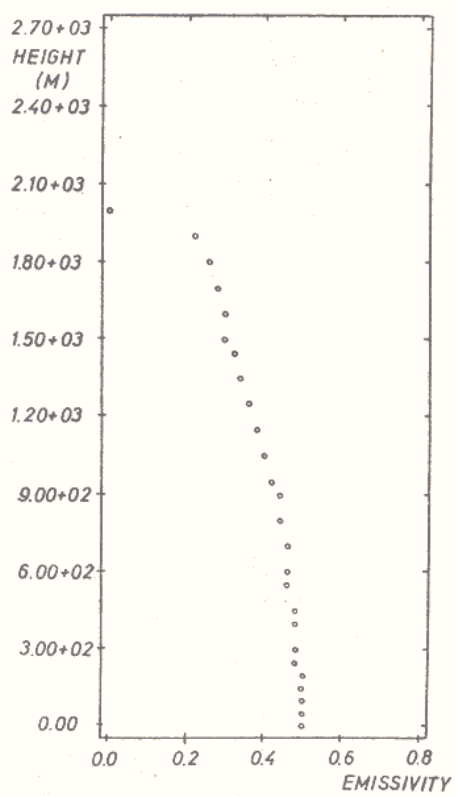

Figure 4. Emissivity due to water vapor in the downward corrected mass of water vapor versus height.

$$E(u) = \begin{cases} 0.133 \log_{10}(1 + 12.6\,u), & \log_{10} u \leq -4 \\ 0.104 \log_{10}(u) + 0.440, & -4 < \log_{10} u \leq -3 \\ 0.121 \log_{10}(u) + 0.491, & -3 < \log_{10} u \leq -1.5 \\ 0.146 \log_{10}(u) + 0.527, & -1.5 < \log_{10} u \leq -1.0 \\ 0.161 \log_{10}(u) + 0.542, & -1.0 < \log_{10} u \leq 0.0 \\ 0.136 \log_{10}(u) + 0.542, & \log_{10} u \leq 0.0 \end{cases}$$

Function u has been defined before (Section 2, eq. (3)). Dimension of u is (g/cm^2).

The form of $E(u_i)$ is: $E(u_i) = a_i \log_{10}(\delta_{ik} + b_i u_i) + c_i$, where δ_{ik} is the Cronecker's symbol. Than it follows:

$$\frac{dE(u_i)}{du_i} = \frac{a_i b_i \log 10\, e}{\delta_{ik} + b_i u_i}$$

and we can obtain:

$$\frac{dE(u_i)}{du_i}, \quad \frac{dE(u_i - u_{j-1/2})}{du_i}, \quad \frac{dE(u_{j+1/2} - u_i)}{du_i}$$

for adequate choice of u_i.

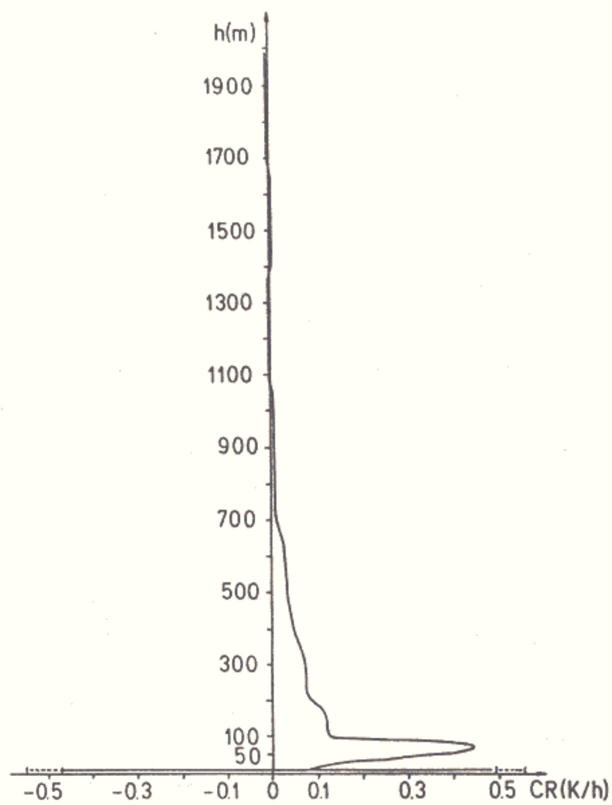

Figure 5. Radiative cooling rate extrapolated for an hour (Wangara night 33-34).

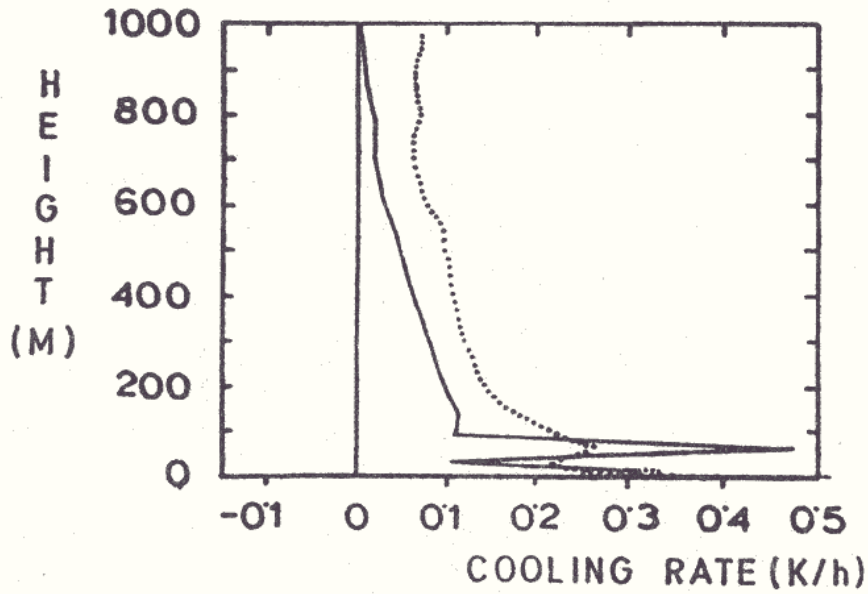

Figure 6. Radiative cooling rate of the present model (solid line) compared to the results of André and Mahrt (1982) (dotted line).

References

André, J. C., G. De Moor, P. Lacarrére, G. Therry and R. du Vachat (1978): Modeling the 24 hour evolution of the mean and turbulent structures of the planetary boundary layer. Journal of the Atmospheric Sciences, **35**, 1861-1883.

André, J. C. and L. Mahrt (1982): The nocturnal surface inversion and influence of clear - air radiative cooling. Journal of the Atmospheric Sciences, **39**, 864-878.

Anfossi, D., P. Bacci and A. Longhetto (1976): Forecasting of vertical temperature profiles in the atmosphere during nocturnal radiation inversions from air temperature trend at screen height. Quarterly Journal of the Royal Meteorological Society, **102**, 173-180.

Bodin, S. (1978): Applied Numerical Modeling of the Atmospheric Boundary Layer. SMHI Rapporter, Undervisning Nr RU 15, 151pp.

Brost, R. A., J. C. Wyngaard (1978): A model study of the stably-stratified planetary boundary layer. Journal of the Atmospheric Sciences, **35**, 1427-1440.

Brunt, D. (1934); Physical and Dynamical Meteorology. Cambridge University Press, 124-146.

Businger, J. A., J. C. Wyngaard, Y. Izumi and E. F. Bradley (1971): Flux-profile relationships in the atmospheric surface layer. Journal of the Atmospheric Sciences, **28**, 181-189.

Clarke, R. H., A. J. Dyer, R. R. Brook, D. G. Reid and A. Troup (1971): The Wangara Experiment: Boundary layer data. Technical Papers **19**, Department of Meteorology and Physics, CSIRO, Melbourne, Australia, 363 pp.

Delage, Y. (1974): A numerical study of the nocturnal atmospheric boundary layer. Quarterly Journal of the Royal Meteorological Society, **100**, 351-364.

Garratt, J. R. and R. A. Brost (1982): Radiative cooling effects within and above the nocturnal boundary layer. Journal of the Atmospheric Sciences, **38**, 2730-2746.

Houghton, J. T. (1977): The Physics of Atmospheres. Cambridge University Press, 134-145.

Klöppel, M., G. Stilke and C. Wamser (1978): Experimental investigations into variations and comparisons with results of simple boundary layer models. Boundary - Layer Meteorology, **15**, 135-146.

Kondratyev, K. Ya. (1972): Radiation Processes in the Atmosphere. Geneva, WMO No. 309, 214 pp.

Nieuwstadt, F.T.M. (1980): A rate equation height in a nocturnal boundary layer. Journal of the Applied Meteorology, **19**, 1445-1447.

Paltridge, G. W. and C. M. R. Platt (1976): Radiative Processes in Meteorology and Climatology. Elsevier, 318 pp.

Pielke, R. A. (1984): Mesoscale Meteorological Modeling. Academic Press, 612 pp.

Wyngaard, J. C. (1975): Modeling the planetary boundary layer. Extension to the stable case. Boundary - Layer Meteorology, **9**, 441-460.

Yamada, T. and G. L. Mellor (1975): A simulation of the Wangara atmospheric boundary layer data. Journal of the Atmospheric Sciences, **32**, 2309-2329.

Zeman, O. (1979): Parameterization of the dynamics of stable boundary layers flow and nocturnal jets. Journal of the Atmospheric Sciences, **36**, 792-804.